Experimental Study on T-Joint of Friction Stir Welding on AA 1065 Aluminum Alloy

[1]Rajankumar Belani, [2]T.Prabakaran
[1]PG Scholar, [2]Assistant Professor
Department of Mechanical Engineering
[1, 2] M.I.E.T. Engineering College, Tiruchirapalli, India

Abstract **- Friction stir welding (FSW) is a solid state joining process for joining high conductivity materials like aluminum and its alloys. In the present study T-joint at various parameters were produced by the friction stir welding. Some parameter provides defect free joints while the other parameters show defects. The tool pin is used in all the parameter is helical shaped. T-joints of AA 1065 aluminum alloy is made without defects. Experimentation will be carried out by changing principle parameters of FSW process. Macro and micro images of traverse section of the weld were captured and analyzed to identify the defects and the bead geometry values were found out using macro images. Most of the defects occur at advancing side at top side of the weld joint. The liquid penetrant inspection (LPI) test was performed for all the joints and no surface cracks were formed on weld line. Scanning electron microscopy (SEM) with Energy dispersive X-ray spectroscopy (EDS) spectra was taken at various weld zones, which shows the topography of welded zone and oxides formation. Tensile properties and micro hardness of the joints were experimentally evaluated for joints formed at different process parameters.**

Index Terms **-Friction stir welding, Aluminum alloy, Defects, Tensile property**

I. INTRODUCTION

FSW process was invented at The Welding Institute (TWI) of UK in 1991 as a solid state joining technique, and it was initially applied to aluminum alloys[1-2]. The basic concept of FSW is remarkably simple. A non-consumable rotating tool with specially designed pin and shoulder is inserted in to the abutting edges of sheets or plates to be joined and traversed along the line of joint. The tool serves two primary functions (a) heating of work piece, and (b) movement of material to produce the joint. The heating is accomplished by friction between the tool and the work piece and plastic deformation of work piece. The localized heating soften the material around the pin and the combination of tool rotation and translation leads to movement of material from the front of pin to the back of pin. As a result of this process a joint is produced in a Solid State. Because of various geometrical features of tools, the material movement around the pin can be quite complex [3].During FSW process, the material under goes intense plastic deformations at elevated temperature, resulting in generation of fine and equi-axed recrystallized grains [4-7].The fine micro structure in friction stir welds produces good mechanical properties.

FSW is considered to be the most significant development in metal joining in a decade and is a “green” technology due to its energy efficiency, environmental friendliness and versatility [8].As compared to conventional welding methods, FSW consumes considerably less energy. No cover gas or flux is used, thereby making the process environment friendly. The joining does not involve use of any filler metal and therefore any aluminum alloy can be joined without concern of compatibility of composition, which is an issue in fusion welding. When desirable, dissimilar aluminum alloys and composites can be joined with equal ease. In contrast to the traditional friction welding, which is usually performed on small axisymmetric parts that can be rotated and pushed against each other to form a joint, friction stir welding can be applied to various type of joints like butt joints, lap joints, T butt joints and fillet joints[8-10].

II. THE EXPERIMENTAL INVESTIGATION

The base material (BM) used for the Experiment was AA 1065 aluminum alloy. Rolled plates of AA 1065 aluminum alloy samples with dimension of 250 mm x 60 mm x 15 mm thick were cut from plates for welding. Before the welding experiment, the surfaces of the plates were grinded with abrasive paper to remove oxidation films and cleaned with alcohol. The material having properties values such as Thermal conductivity 218W/m-˚K, Tensile strength 110 MPa, Yield strength 105 MPa and 13 % of Elongation. Typical chemical composition of material listed in Table 1.

Table 1. Typical chemical composition of material

Elements	Al	Cu	Fe	Mg	Mn	Si	Ti	Zn	V
Wt%	99.68	0.001	0.196	---	0.0033	0.047	---	0.002	---

FSW process experimental set up with two plates set at right angle and clamped with bed by using special fixture, as shown in Fig.1. The details about welding process, as shown in Fig.2. A cylindrical taper tool with tri-flutes, scrolled shoulder and with fins, as shown in Fig. 3, made of high speed steel (18% W, 4% Cr, 1% V) with pin length of 15.5mm was used. The tool was subjected to oil quenching and tempering to get 50 HRC. The pin and shoulder diameters of the tool are 14.5 mm and 40 mm

respectively. An angle of 6˚ was designed between the horizontal planes of the shoulder to impart the forging action. The samples were subjected to single pass of FSW with different parameters listed in Table 2.

Fig.1. Experimental set up of process

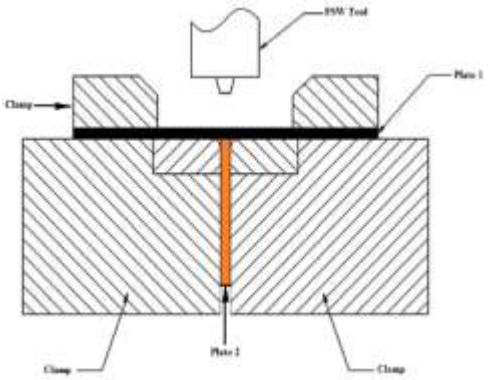

Fig.2. Schematic diagram of welding process

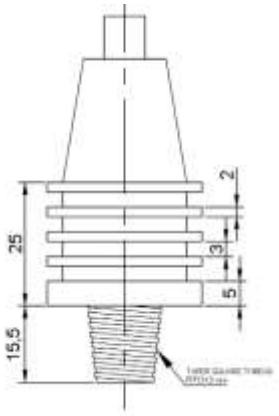

Fig.3. Schematic diagram of FSW tool

Table 2. Investigated case studies

Joint No.	Pin Shape	Rotational Speed (rpm)	Traverse Speed (mm/min)	Tool Length (mm)	Pin Depth (mm)
1A	Elliptical	220	20	105.5	15.5
2A	Elliptical	320	25	105.5	15.5
3A	Elliptical	320	20	105.5	15.5
6F	Elliptical	450	25	105.5	15.5
6A	Elliptical	500	20	105.5	15.5

Microstructure studies were carried out by visually. The sample were polished with emery paper up to 500 grade and then etched. The etchant used for micro structural analysis have following composition: 75 ml of HCL and 25 ml of water. The etchant time used was 30 to 60 seconds. Micro structural studies was carried out by optical and SEM of the cross sections perpendicular to the tool traverse direction to analyze the grain sizes at various zones of the welded joints. The samples were mirror polished & properly etched. The etchant used for micro structural analysis have following composition: 50 ml Poultons Reagent, 25 ml HNO_3 and 40 ml solution of 3g chromic acid per 10 ml of water. The composition of Poultons Reagent is 1 ml HCL, 6 ml HNO_3, 1 ml HF and 1 ml water. The etching time used was 15-20 seconds.

The Vickers micro hardness values of AA 1065 after FSW and BM were measured using a load of 200g and 15s. EDS analysis was carried out to check micro level chemical composition and element mapping. LPI also done for all the samples for crack and any surface defects were investigated. Mechanical testing was done by universal testing machine UTE-40. The welded joints are sliced using power hacksaw and then machined according to American society for testing and materials (ASTM) A370 standards, as shown in Fig.4. Tensile test has been carried out in 100 kN; specimen is loaded at the rate of 1.5 kN/ min as per ASTM specifications. The 0.2% offset yield strength; ultimate tensile strength and percentage of elongation have been evaluated.

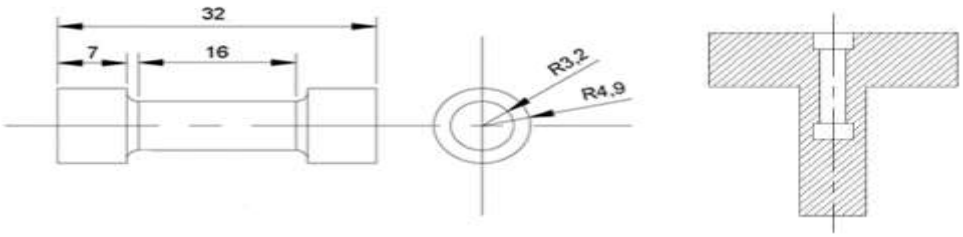

Fig.4. Schematic diagram of tensile test specimen preparation

III. RESULTS AND DISCUSSION

i. Microstructure Characterization

Standard metallographic techniques are followed and the microstructure of friction stir welded plates are examined. The defect free welded T-joints with parameters 320rpm/20feed rate (Joint 3A) and 320rpm/25feed rate (Joint 2A), as shown in Fig.5. It is clear that there is sufficient heat for metal flow of defect free joint formation. The observed micro structure of the T-joints is consistent with those reported by others on aluminum alloys [11].The plate revealed classical nugget structure quite similar to observation in classical welding techniques, and contained the presence of overlapping circular ring like features. A polished cross section in the plane will intersect the successive circular revolutions to produce the 'onion rings'. The 'onion ring 'like features found in the weld zone are an evidence of the characteristic material transport occurring during friction stir welding. A simple extrusion of one layer of semi-cylinder during one full rotation of the tool and a cross sectional slice taken through such a semi-cylinder reveals an 'onion ring' patter is well aided by a reflection of material flow at the imaginary walls of the groove that does exist for the situation of regular milling of the metal[12]. An insight in to the mechanism of 'onion ring' formation would facilitate an understanding of material flow during FSW. A tunnel defect due to complex metal flow pattern is found in joint 1A.The metal flow lines are visible. These types of defects were occurred by may be the insufficient heat input and abnormal stirring. At lower parameters causes the different streams of metal flow at top side of the advantage side. In the joint 6A sample the cavity defect is formed at advancing side due to insufficient metal flow. In the joint 6F sample cavity defect at the interface of the Nugget and TMAZ due to insufficient metal flow at the top side of the joint and complete filling of metal at bottom side of the joint are observed in macrostructure. At joint portion the surface cracks were formed because of the insufficient contact force.

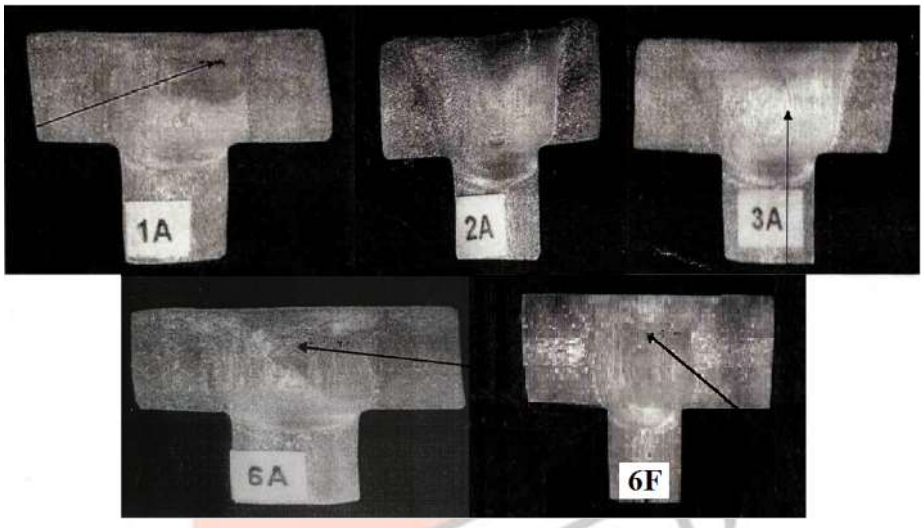

Fig.5. Macrographs on cross-sections of all the experimental FSWed T-joints
(Joint 1A Tunnel defect, Joint 3A Onion ring formation, Joint 6A Cavity defect, Joint 6F Cavity and Neck crack defect)

ii. Micro-hardness Profile

Hardness values are taken in parallel to flange of the T-joint as shown in Fig.6. Hardness profile was plotted on cross sections perpendicular to the tool traverse directions. Hardness distributions in the FSW Heat affected zone (HAZ) are complex .In the present study shows the existence of three regions for each. These are the Nugget zone (NZ), from the Plate joint line(PJL) extending 5-6mm out, the Thermo-mechanically affected zone (TMAZ) from 5-6mm to 10-12mm to and the HAZ from 10-12mm to 30-45mm.Each region has qualitatively distinct values of hardness .The NZ has a fine recrystallized grain structure, with hardness values between 30 and 40Hv1.outside the nugget, the TMAZ consists of highly elongated and deformed grains ,which comprise the softest (20-30Hv1) part of the HAZ. Beyond 10-12mm from the PJL the structures is only heat affected and contains a parent plate grain structure.

Investigation shows that tool rotation speed 500rpm and feed rate 20mm/min (Joint 6A) the hardness of the FSW samples is high as compared to lower parameters, as shown in Fig.7. The influence of traverse speed in hardness is less compared to that of tool rotation speed. In case of AA 1065 alloy, the hardness are mainly depends on the grain size and the dislocation density. Hence, the hardness of FSW samples primarily depends on the grain size. The grain refinement is more at low tool rotation speeds, as heat generated is low; it is expected to get high hardness at low rpm. The hardness at advancing side is slightly higher than retreating side. The hardness at the bottom of weld is higher than value compared to top surface because more cooling rate at the bottom side of the joint.

It is noted that as tool rotation speed 320rpm and feed rate 25mm/min (Joint 2A) the hardness of the FSW samples is high as compared to lower parameters, as shown in Fig.8. In this case also the hardness values at bottom side of joints are higher than the top side of the joint. These parameters gave higher hardness web corners compared to center of the joint.

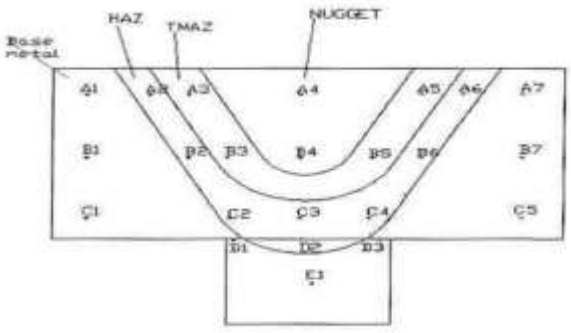

Fig.6. Schematic diagram shows hardness measured points

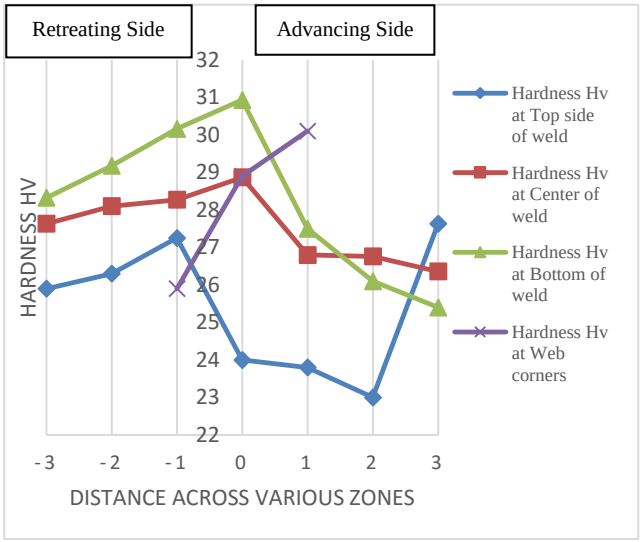

Fig.7. Micro hardness profile of Joint 6A

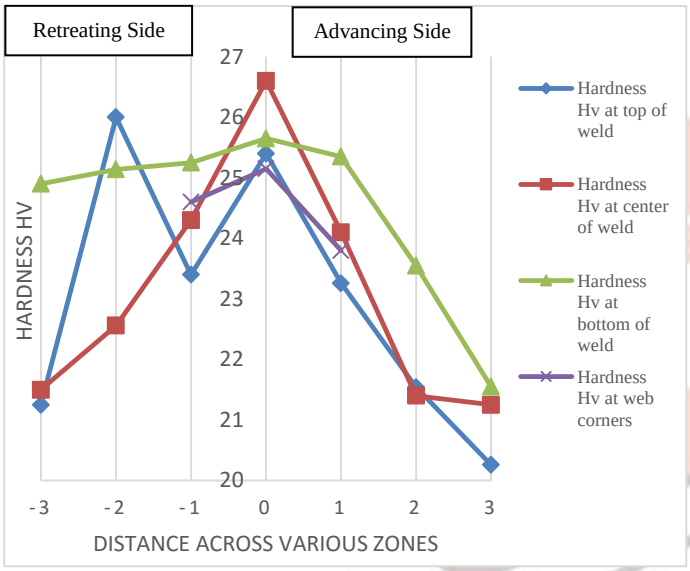

Fig.8. Micro hardness profile of Joint 2A

Fig.9. Micro hardness profile of Joint 3A

On the BM zone the elongated grains were observed the heat associated with welding changes the microstructure of the material HV min and HV max represent the hardness in the solution- treated and crystallization. The effect of welding is to cause a drop in hardness from HV max towards HV min as the peak temperature experienced increases. This is because grains will coarsen and reduce in number density in regions remote from heat source, and will re-enter solution when the peak temperature is sufficiently high [13]. Some changes may occur during the cooling part of thermo cycle, resulting in hardness value beyond HV min, ultimate result is a minimum in hardness somewhere in HAZ and TMAZ due to the competing effects of dissolution and recrystallization has taken place during the friction stir welding [14]. The transformation of initial elongated grain structure into fine equi axed grains in the weld nugget is reported to be dynamic recrystallization so the hardness is higher than the other zones we observed. [16-19]

Investigation result shows that as tool rotation speed 320rpm and feed rate 20mm/min (Joint 3A) the hardness of the FSW samples is high as compared to lower parameters as shown in Fig.9. In this case also the hardness values at top side of joints are higher than the bottom side of the joint. These parameters gave hardness values web corners is slightly higher than the center of joint, because of at corners higher cooling rates than the center portion of the joint.

Also the hardness distribution is not symmetric with respect to the tool rotation axis. Along the cross section perpendicular to the tool traverse direction of the FSW specimens, the hardness would be more at the advancing side compared to the retreating side.

iii. Tensile Testing

Traverse tensile properties such as yield strength, tensile strength, percentage of elongation and percentage of reduction of joint have been evaluated. For each process parameters one specimen is tested, as shown in Fig.11. From the results, it can be inferred that the rotational speed and traverse speed are having influence on tensile properties of the T-Joints. The room temperature tensile properties are summarized in Table 3.The results reported are the mean values based on duplicate tests. The yield strength and ultimate tensile strength of samples are cut traverse to the weld direction to include the weld direction to include the weld zone at the center of the machined test sampled are superior to the welded Al AA1065 counterpart. The maximum yield strength of the FSW sample 56 N/mm^2 and then decreases again with highest speeds, revealing strong hardening phenomena to take place over a certain tool advantage speed limit with respect to unwelded counterpart, while the tensile strength is as high as for sample 2A is 78.79 N/mm^2 taken from the friction stir welded samples from both flange and web failed at BM only. This is attributed to the effect arising from localization of strain occurring in BM softened resulting in a comparatively high overall strain to failure elongation in friction stir welded process [15]. The material ductility seems to follow the same behavior and optimal mechanical properties with elongation equal to 30% are achieved around 20mm/min tool speed value, after which a sensible ductility reduction appears.

The tensile strength and yield strength variation is shown in Fig.10 and same with all the properties. At the lower process parameters were given slightly higher values than higher process parameters. Likewise % elongation has shown the similar results. L pull test also carried out, as shown in Fig.12.After testing the failure occurred at BM for all joints, as shown in Fig.13.

Table 3. Mechanical properties of Joints.

Joint no.	Tensile Strength (N/mm^2)	Yield Strength (N/mm^2)	% elongation	% Reduction area
1A	75.38	50	30	89
2A	78.79	48	25	76
3A	77.07	56	25	84
6F	74.87	53	26.5	88.5
6A	73.14	49	25	83.5

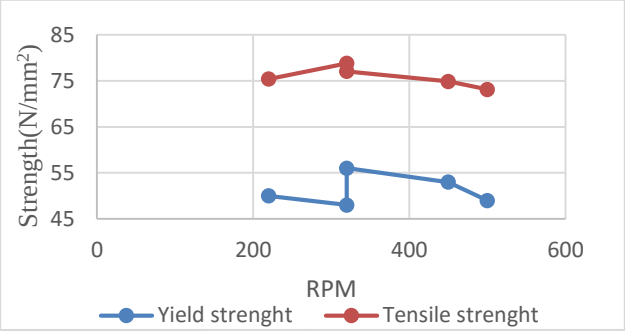

Fig.10. Schematic diagram of tensile tests

Fig.11. Tensile tested specimen

Fig.12 Schematic diagram of L pull tests.

Fig.13. L pull tested specimen

iv. Liquid Penetrate Inspection (LPI)

In all FSW joint LPI test performed and found satisfactory. The red developer is used for detecting the cavities and surfaces cracks. No red indication is formed on the weld line. So that joint on weld line is perfect.

v. Optical Microscopy Analysis

Microstructural studies were carried out by using optical across the cross section perpendicular to the tool traverse direction to analyse the grain size across the various zones of welded joints. On the BM zone the elongated grains are observed. Microstructure analysis was done for various conditions of welding speed and feed rate. In all the welding conditions, the flow of material inside the nugget is evidence of substantial plastic stirring during FSW. The micrographs of the centre of the NZs of a sample joined by employing a welding speed of 20mm/min are, as shown in Fig.14. The microstructure of the material appears as very fine and equi axed grains in all welding conditions as can be noted by the difference with standing microstructure revealing the classical elongated grains belonging to the rolling operations. A strong difference in grain size and distributions was observed for different ranges of travel speed; by increasing the travel speed it seems that the combinations between hot working and dynamic recovery and recrystallization is optimal for chosen conditions. A strong variation in mean grain size was observed by increasing the

advantages speed from 16 to 25mm/min up to a plateau corresponding to no further variations by increasing the speed up to 40mm/min. This is typical for aluminum alloys in which the nugget mean grain size decrease with increasing travel speed, at the given rotation speed, up to the minimum and after it starts to increase again.

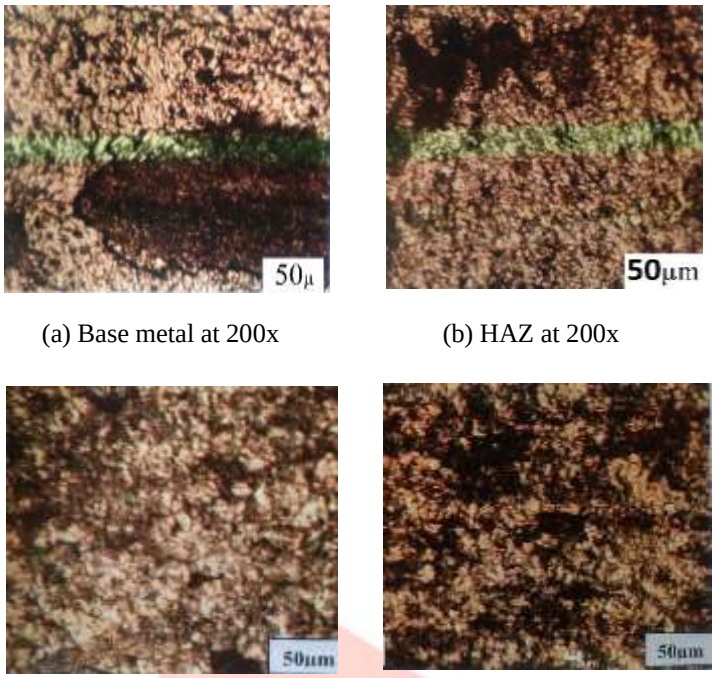

(a) Base metal at 200x (b) HAZ at 200x

(c) TMAZ at 100x (d) Nugget at 200x

Fig.14. The microstructure of a AA 1065 T-joint (Joint 1A case study)

It was observed that there is an increase in the peak temperature with increasing the revolutionary pitch and a strong effect of travel speed on the material mixing; for this reason it was important to couple such parameters to the resultant mean grain size. By decreasing the temperature in the NZ the force acting on the material is not able to produce a plastic flow the proper of a continuous dynamic recrystallization process, while by increasing the temperature of material for travel speed too low for used welding speed the material is extremely softened and can be subjected to grain growth after deformation.

vi. SEM Analysis

These SEM images reveal that there was a variation in grain size from the BM to various zones of the welded zones. The grains on the nugget were found to be finer than that of the others zones.

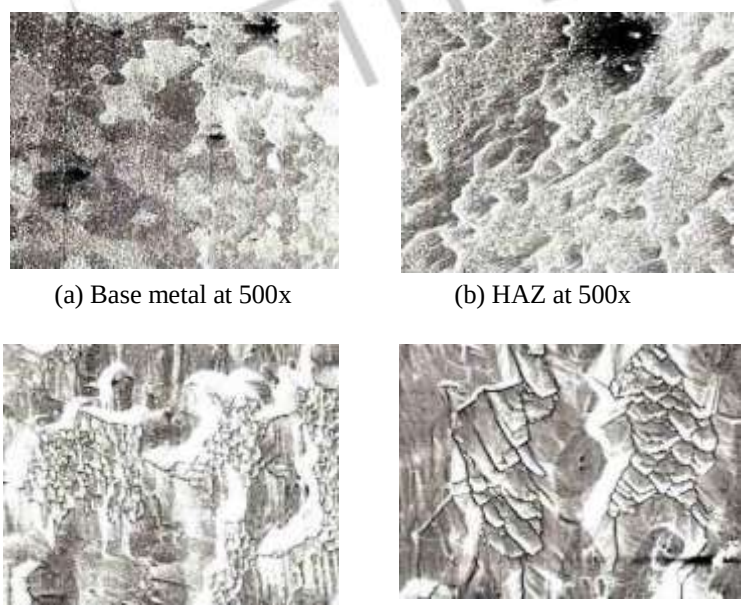

(a) Base metal at 500x (b) HAZ at 500x

(c) TMAZ at 500x (d) Nugget at 500x

Fig.15. SEM images of the surfaces in four different regions of Joint 3A

The kissing bond region was observed that there was a close match between the interlayer distance and the traverse speed. This suggest that the heat generation of FSW process could not produce sufficient frictional force and heat for NZ at 320rpm and 20 feed rates .Moreover , with the increase of the contact state variable a friction interface conditions where the pin surface and weld material are mainly sticking. It is considered that in the welding process, the nugget grain did not experience high temperature and violent plastic formation. As a result the nugget and TMAZ has poor properties in the weld.

vii. EDS Analysis

Fig.16 Morphology at TMAZ of Joint 2A

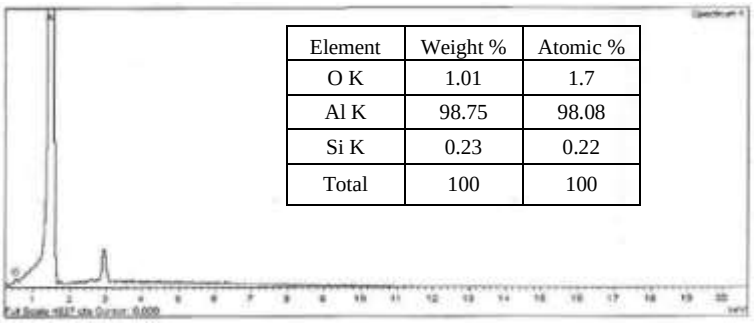

Element	Weight %	Atomic %
O K	1.01	1.7
Al K	98.75	98.08
Si K	0.23	0.22
Total	100	100

Fig.17 Composition at TMAZ of Joint 2A

EDS was utilized to identify the phases present in the TMAZ sliced specimens from aluminum alloy AA 1065. Two peaks, one large peak is aluminum and another one is silicon & oxides observed as shown in Fig. 17. Those only a few particles are located at the grain boundary while many others have been in matrix as shown in Fig. 16. From the EDS analysis it was found that the particles are likely Al_2O_3 particles. It is well known that the amorphous oxide particles of AA 1065 aluminum alloy are easily substituted by the crystalline structure under long time thermal cycling. However, FSW is a welding process with relatively rapid heating and cooling resulting in no sufficient heat input for formation of the amorphous structures. Therefore, the amorphous oxide particles could not change into crystalline phases.

IV. CONCLUSION

The visual macrograph of friction stir welded aluminum alloys revealed different types of defects at different regions. Friction stir weld defects can classified (a) Cavity or groove like defects due to insufficient metal flow. (b)Tunnel defects due to abnormal stirring. (c)Neck cracks due to less compressive force of the tool shoulder at contact surface.

1. Most of the above defects were due to insufficient metal flow because of low heat input and abnormal stirring, which is caused due to the different temperatures between the upper part near the surface and lower part.
2. Different geometric values are possible at different process parameters.
3. Micro hardness test reveals hardness across the NZ which various for most of the samples. The hardness of the advantage side is greater than that of the retreating side.
4. The micro structural analysis was revealed that coarse grains HAZ zones where as fine grains at weld NZ.
5. SEM analysis was carried out at various zones, it was shown that pores at BM and kissing bond defects at HAZ whereas fine equi axed grains was observed NZ.
6. EDS analysis was carried at TMAZ shown that oxide layer rich in Al_2O_3.
7. Tensile strength values clearly indicate that FSW is very effective technique to fabricate T-joints with aluminum AA 1065 alloy.

REFERENCES

[1] W.M. Thomas, E.D. Nicholas, J.C. Needham, M.G. Murch, P. Templesmith, C.J. Dawes, G.B. Patent Application No. 9125978.8 ,December 1991.
[2] C. Dawes, W. Thomas, TWI Bulletin 6, November/December 1995, p. 124.
[3] B. London, M. Mahoney, B. Bingel, M. Calabrese, D.Waldron, in: Proceedings of the Third International Symposium on Friction Stir Welding, Kobe, Japan,27–28 September, 2001.
[4] C.G. Rhodes, M.W. Mahoney, W.H. Bingel, R.A. Spurling, C.C. Bampton, Scripta Mater. 36 (1997) 69.
[5] G. Liu, L.E. Murr, C.S. Niou, J.C. McClure, F.R. Vega, Scripta Mater. 37 (1997) 355.
[6] K.V. Jata, S.L. Semiatin, Scripta Mater. 43 (2000) 743.
[7] S. Benavides, Y. Li, L.E. Murr, D. Brown, J.C. McClure, Scripta Mater. 41 (1999) 809.
[8] L.E. Murr, Y. Li, R.D. Flores, E.A. Trillo, J.C. McClure, Mater. Res. Innovat., 2 (1998), 150.
[9]Y. Li, E. A. Trillo, L. E. Murr, J. Mater. Sci. Lett. 19, (2000), p. 1047.
[10]Y. Li, L. E. Murr, J. C. McClure, Mater. Sci. Eng. A271, (1999), pp. 213-223.
[11]K.N. Krishnan: Mater. Sci. and Eng., 327, 2002 pp. 246
[12] G. Biallas, G. Braun, C.D. Donne, G. Staniek, W. Kaysser, Mechanical properties and corrosion behavior of friction stir welded 2024-T4; Proceedings of the 1st International Symposium Friction Stir Welding, TWI, (1999)

[13]Y.S.Sato, H. Kokawa, M. Enomoto, S. Jogan, Microstructural evolution of 6063 aluminum during friction-stir welding; Metall. Mater. Trans. A 1999; 30(9):2429–37
[14]Grong Ø. Metallurgical modelling of welding. 2nd ed. London: Maney; 1997
[15]T.S. Srivatsana, S. Vasudevana, L. Parkb, The tensile deformation and fracture behavior of friction stir welded aluminum alloy 2024; Mater. Sci. and Eng. A 2007; 466:235-45.
[16]I. Shigematsu, Y. J. Kwon, K. Suzuki, T. Imai, and N. Saito, Joining of 5083 and 6061 aluminum alloys by friction stir welding; J. Mater. Sci. Lett., vol. 22, no. 5, pp. 353–356, 2003
[17]S. Muthukumaran, S. K Mukherjee, Two Modes of Metal Flow Phenomenon in Friction Stir Welding; Science and Technology of Welding and Joining, 11, (2006), 337-340.
[18]S. Benavides, Y. Li, L. E. Murr, D. Brown and J. C. McClure, "Low-Temperature Friction-stir Welding of 2024 Aluminum," Scripta Materialia, Vol. 41, No. 8, 1999, pp. 809-815
[19]B. London, M. Mahoney, W. Bingel, M. Calabrese, RH Bossi, D. Waldron, Material flow in friction stir welding monitored with Al–SiC and Al–W composite markers; In: Proceedings of the Symposium on Friction Stir Welding and Processing II, Warrendale, PA, TMS, 2003.